white matter including a thin corpus callosum, mild brain atrophy, and mild cerebellar hypoplasia are frequently seen in patients with mutations in other genes involved in the biosynthesis of the GPI anchor, such as *PIGN*, *PGAP2*, *DPM1*, and *DPM2*,[10,15,23,24] high signals on DWI have never been reported. In addition, the ADC map showed adversely low or decreased signals, suggesting restricted water diffusion. This pattern (a high DWI signal and low ADC values) can be seen in patients with specific metabolic disorders, such as nonketotic hyperglycinemia, phenylketonuria, maple syrup urine disease, Leigh encephalopathy, infantile neuroaxonal dystrophy, Wilson disease, metachromatic leukodystrophy, and Canavan disease.[25] Indeed, metabolic disorders, particularly nonketotic hyperglycinemia, are strongly associated with EME, which is common in patients with *PIGA* mutations. A brain MRI of a patient in early infancy with a recently reported *PIGO* deficiency also showed hypomyelination and abnormally high signals in T2-weighted images from the bilateral basal ganglia to the brainstem.[26] While the pathologic mechanism for restricted diffusion patterns in specific areas is unknown, this finding may be useful to screen patients with a GPI deficiency.

Patients with the severe type of *PIGA* mutation showed both an asymmetrical and symmetrical pattern of suppression burst on EEG in this study. The suppression burst pattern is characteristic for 2 types of EOEE, OS and EME, and most patients of both disorders show a symmetrical pattern. The asymmetrical pattern has been reported in patients with agenesis of the corpus callosum such as Aicardi syndrome,[27] and *KCNQ2* mutations.[4] All 3 patients with the asymmetrical suppression burst in the present study also showed white matter immaturity with a thin corpus callosum and abnormally high signals in deep white matter on DWI. These data indicate a disturbed connectivity of the bilateral hemisphere in patients with *PIGA* mutations. The adverse advancement of the EEG findings from hypsarrhythmia to suppression burst in our cases, which is usually observed in neonates, might reflect the retrogression of brain function, which is also seen in the progression of brain atrophy.

Patient 1 showed severe hydronephrosis caused by the vesicoureteral reflux and hepatoblastoma, so a diagnosis of Schinzel-Giedion syndrome was made. This is an autosomal dominant disorder characterized by severe developmental delay, distinctive facial features with a prominent forehead, midface retraction, short, upturned nose, and either hydronephrosis or typical skeletal malformations, such as sclerotic skull base, wide occipital synchondrosis, increased cortical density or thickness, and broad ribs.[28] *SETBP1* mutations have been reported in patients with Schinzel-Giedion syndrome[29] but were not identified in our patient. Because of the phenotypic similarities between patients with *PIGA* mutation and those with Schinzel-Giedion syndrome, we suggest that patients with Schinzel-Giedion syndrome with no *SETBP1* mutations should undergo genetic analysis of their *PIGA* gene or other genes involved in the biosynthesis of the GPI anchor.

Patients with mutations in *PIGL*, *PIGM*, *PIGN*, *PIGO*, *PIGT*, *DPM2*, and *MPDU1* often die in early childhood.[9,12,14–16,23,30] While pneumonia is the main cause of death in these patients, intractable seizures, which rigorously worsen the prognosis of life expectancy and cognitive function, frequently occur. It is of interest that the targeted agents butyrate and pyridoxine were reported to be effective for seizure treatment in patients with *PIGM* or *PIGO* mutation, respectively.[26,31] However, patient 5 in this study did not respond to pyridoxine. The study of more patients will facilitate the establishment of personalized treatment methods for patients with GPI deficiencies.

Our study demonstrated that mutations in *PIGA* are causative for a variety of EOEEs, particularly for patients with myoclonus and asymmetrical suppression burst on EEG. Multiple anomalies with facial dysmorphism resembling Schinzel-Giedion syndrome, delayed myelination with restricted diffusion patterns at the brainstem, and deep white matter are key findings in a severe form in patients with *PIGA* mutations. Nevertheless, a wide range of clinical phenotypes of *PIGA* mutations should be kept in mind, including the less severe forms involving intellectual disability and treatable seizures without facial dysmorphism.

AUTHOR CONTRIBUTIONS

Mitsuhiro Kato: study concept and design, analysis of the clinical data, interpretation of the data, and drafting/revising of the manuscript. Hirotomo Saitsu: study concept and design, analysis of the genetic data, interpretation of the data, and drafting/revising of the manuscript. Yoshiko Murakami: study concept and design, analysis of the biological data, interpretation of the data, and drafting/revising of the manuscript. Kenjiro Kikuchi, Shuei Watanabe, Mizue Iai, Kazushi Miya, Ryuki Matsuura, and Rumiko Takayama: analysis of the clinical data and sample collection. Chihiro Ohba, Mitsuko Nakashima, Yoshinori Tsurusaki, and Noriko Miyake: analysis of the genetic data. Shin-ichiro Hamano and Hitoshi Osaka: analysis of the clinical data and sample collection. Kiyoshi Hayasaka: analysis of the clinical data and revising of the manuscript. Taroh Kinoshita: analysis of the biological data, interpretation of the data, and drafting/revising of the manuscript. Naomichi Matsumoto: study concept and design, analysis of the genetic data, interpretation of the data, and drafting/revising of the manuscript.

ACKNOWLEDGMENT

The authors are grateful to the patients and their families for their participation in this study. The authors thank Keiko Tanaka, Kana Miyanagi, Nobuko Watanabe, and Kiyomi Masuko for their technical assistance.

STUDY FUNDING

This study was supported by the Ministry of Health, Labour and Welfare of Japan (25140101, 24133701,11103577, 11103340, 10103235), a Grant-in-Aid for Scientific Research (A), (B), and (C) from the Japan

Society for the Promotion of Science (A: 24249019, B: 25293085 25293235, C: 24591500, 23590363), the Takeda Science Foundation, the fund for Creation of Innovation Centers for Advanced Interdisciplinary Research Areas Program in the Project for Developing Innovation Systems, the Strategic Research Program for Brain Sciences (11105137), and a Grant-in-Aid for Scientific Research on Innovative Areas (transcription cycle, exploring molecular basis for brain diseases based on personal genomics) from the Ministry of Education, Culture, Sports, Science and Technology of Japan (12024421, 25129705).

DISCLOSURE

M. Kato is funded by research grants from the Ministry of Health, Labour and Welfare of Japan, and a Grant-in-Aid for Scientific Research (C) from the Japan Society for the Promotion of Science. H. Saitsu is funded by a Grant-in-Aid for Scientific Research (B) from the Japan Society for the Promotion of Science, and the Takeda Science Foundation. Y. Murakami is funded by a Grant-in-Aid for Scientific Research (C) from the Japan Society for the Promotion of Science, the Takeda Science Foundation, a Grant-in-Aid for Scientific Research on Innovative Areas (exploring molecular basis for brain diseases based on personal genomics) from the Ministry of Education, Culture, Sports, Science and Technology of Japan. K. Kikuchi, S. Watanabe, M. Iai, K. Miya, R. Matsuura, R. Takayama, C. Ohba, M. Nakashima, and Y. Tsurusaki report no disclosures relevant to the manuscript. N. Miyake is funded by research grants from the Ministry of Health, Labour and Welfare of Japan, a Grant-in-Aid for Scientific Research (B) from the Japan Society for the Promotion of Science, and the Takeda Science Foundation. S. Hamano, H. Osaka, and K. Hayasaka report no disclosures relevant to the manuscript. T. Kinoshita is supported by a Grant-in-Aid for Scientific Research (A) from the Japan Society for the Promotion of Science. N. Matsumoto is supported by grants from the Ministry of Health, Labour and Welfare of Japan, a Grant-in-Aid for Scientific Research (A) from the Japan Society for the Promotion of Science, the Takeda Science Foundation, the fund for Creation of Innovation Centers for Advanced Interdisciplinary Research Areas Program in the Project for Developing Innovation Systems, the Strategic Research Program for Brain Sciences, a Grant-in-Aid for Scientific Research on Innovative Areas (transcription cycle) from the Ministry of Education, Culture, Sports, Science and Technology of Japan. Go to Neurology.org for full disclosures.

Received November 7, 2013. Accepted in final form February 7, 2014.

REFERENCES

1. Kato M, Saitoh S, Kamei A, et al. A longer polyalanine expansion mutation in the *ARX* gene causes early infantile epileptic encephalopathy with suppression-burst pattern (Ohtahara syndrome). Am J Hum Genet 2007;81:361–366.
2. Saitsu H, Kato M, Mizuguchi T, et al. De novo mutations in the gene encoding STXBP1 (MUNC18-1) cause early infantile epileptic encephalopathy. Nat Genet 2008;40: 782–788.
3. Saitsu H, Kato M, Osaka H, et al. *CASK* aberrations in male patients with Ohtahara syndrome and cerebellar hypoplasia. Epilepsia 2012;53:1441–1449.
4. Kato M, Yamagata T, Kubota M, et al. Clinical spectrum of early onset epileptic encephalopathies caused by *KCNQ2* mutation. Epilepsia 2013;54:1282–1287.
5. Nakamura K, Kato M, Osaka H, et al. Clinical spectrum of *SCN2A* mutations expanding to Ohtahara syndrome. Neurology 2013;81:992–998.
6. Kato M. A new paradigm for West syndrome based on molecular and cell biology. Epilepsy Res 2006;70(suppl 1): S87–S95.
7. Saitsu H, Tohyama J, Kumada T, et al. Dominant-negative mutations in alpha-II spectrin cause West syndrome with severe cerebral hypomyelination, spastic quadriplegia, and developmental delay. Am J Hum Genet 2010;86:881–891.
8. Kurian MA, Meyer E, Vassallo G, et al. Phospholipase C beta 1 deficiency is associated with early-onset epileptic encephalopathy. Brain 2010;133:2964–2970.
9. Almeida AM, Murakami Y, Layton DM, et al. Hypomorphic promoter mutation in *PIGM* causes inherited glycosylphosphatidylinositol deficiency. Nat Med 2006;12: 846–851.
10. Hansen L, Tawamie H, Murakami Y, et al. Hypomorphic mutations in *PGAP2*, encoding a GPI-anchor-remodeling protein, cause autosomal-recessive intellectual disability. Am J Hum Genet 2013;92:575–583.
11. Johnston JJ, Gropman AL, Sapp JC, et al. The phenotype of a germline mutation in *PIGA*: the gene somatically mutated in paroxysmal nocturnal hemoglobinuria. Am J Hum Genet 2012;90:295–300.
12. Krawitz PM, Murakami Y, Hecht J, et al. Mutations in *PIGO*, a member of the GPI-anchor-synthesis pathway, cause hyperphosphatasia with mental retardation. Am J Hum Genet 2012;91:146–151.
13. Krawitz PM, Schweiger MR, Rodelsperger C, et al. Identity-by-descent filtering of exome sequence data identifies *PIGV* mutations in hyperphosphatasia mental retardation syndrome. Nat Genet 2010;42:827–829.
14. Kvarnung M, Nilsson D, Lindstrand A, et al. A novel intellectual disability syndrome caused by GPI anchor deficiency due to homozygous mutations in *PIGT*. J Med Genet 2013;50:521–528.
15. Maydan G, Noyman I, Har-Zahav A, et al. Multiple congenital anomalies-hypotonia-seizures syndrome is caused by a mutation in *PIGN*. J Med Genet 2011;48: 383–389.
16. Ng BG, Hackmann K, Jones MA, et al. Mutations in the glycosylphosphatidylinositol gene *PIGL* cause CHIME syndrome. Am J Hum Genet 2012;90:685–688.
17. DePristo MA, Banks E, Poplin R, et al. A framework for variation discovery and genotyping using next-generation DNA sequencing data. Nat Genet 2011; 43:491–498.
18. Saitsu H, Nishimura T, Muramatsu K, et al. De novo mutations in the autophagy gene *WDR45* cause static encephalopathy of childhood with neurodegeneration in adulthood. Nat Genet 2013;45:445–449.
19. Wang K, Li M, Hakonarson H. ANNOVAR: functional annotation of genetic variants from high-throughput sequencing data. Nucleic Acids Res 2010;38:e164.
20. Molinari F, Raas-Rothschild A, Rio M, et al. Impaired mitochondrial glutamate transport in autosomal recessive neonatal myoclonic epilepsy. Am J Hum Genet 2005;76: 334–339.
21. Nozaki M, Ohishi K, Yamada N, Kinoshita T, Nagy A, Takeda J. Developmental abnormalities of glycosylphosphatidylinositol-anchor-deficient embryos revealed by Cre/loxP system. Lab Invest 1999;79:293–299.
22. Watanabe S, Murayama A, Haginoya K, et al. Schinzel-Giedion syndrome: a further cause of early myoclonic encephalopathy and vacuolating myelinopathy. Brain Dev 2012;34:151–155.
23. Barone R, Aiello C, Race V, et al. DPM2-CDG: a muscular dystrophy-dystroglycanopathy syndrome with severe epilepsy. Ann Neurol 2012;72:550–558.
24. Yang AC, Ng BG, Moore SA, et al. Congenital disorder of glycosylation due to *DPM1* mutations presenting with dystroglycanopathy-type congenital muscular dystrophy. Mol Genet Metab 2013;110:345–351.

25. Sener RN. Diffusion magnetic resonance imaging patterns in metabolic and toxic brain disorders. Acta Radiol 2004; 45:561–570.
26. Kuki I, Takahashi Y, Okazaki S, et al. Vitamin B6-responsive epilepsy due to inherited GPI deficiency. Neurology 2013; 81:1467–1469.
27. Aicardi J. Aicardi syndrome. Brain Dev 2005;27: 164–171.
28. Lehman AM, McFadden D, Pugash D, Sangha K, Gibson WT, Patel MS. Schinzel-Giedion syndrome: report of splenopancreatic fusion and proposed diagnostic criteria. Am J Med Genet A 2008;146A: 1299–1306.
29. Hoischen A, van Bon BW, Gilissen C, et al. De novo mutations of *SETBP1* cause Schinzel-Giedion syndrome. Nat Genet 2010;42:483–485.
30. Kranz C, Denecke J, Lehrman MA, et al. A mutation in the human *MPDU1* gene causes congenital disorder of glycosylation type If (CDG-If). J Clin Invest 2001;108:1613–1619.
31. Almeida AM, Murakami Y, Baker A, et al. Targeted therapy for inherited GPI deficiency. N Engl J Med 2007;356: 1641–1647.

CLINICAL GENETICS An International Journal of Genetics, Molecular and Personalized Medicine

Clin Genet 2014: 85: 396–398
Printed in Singapore. All rights reserved

Published by John Wiley & Sons Ltd
CLINICAL GENETICS
doi: 10.1111/cge.12188

Letter to the Editor

AKT3 and *PIK3R2* mutations in two patients with megalencephaly-related syndromes: MCAP and MPPH

To the Editor:

Megalencephaly-capillary malformation syndrome (MCAP) and megalencephaly-polymicrogyria-polyd actyly-hydrocephalus syndrome (MPPH) belong to a spectrum of megalencephaly-related syndromes. The diagnostic criteria for MCAP include megalencephaly plus capillary malformations or syndactyly, and those for MPPH include megalencephaly and polymicrogyria, an absence of vascular anomalies, syndactyly, and brain heterotopia (1). Recently, *AKT3*, *PIK3R2*, and *PIK3CA* mutations have been identified in MCAP and MPPH (2). The proteins encoded by these genes are core components of the phosphatidylinositol 3-kinase (PI3K)-AKT pathway (3). Here, we report two patients with an *AKT3* and *PIK3R2* mutation. The study protocol was approved by the Institutional Review Boards for Ethical Issues at Yokohama City University and Yamagata University.

Patient 1 is an 8-year-old girl who has been previously reported as having MPPH (4). Brain magnetic resonance imaging (MRI) at 6 years showed asymmetry of the gyral pattern, dilated lateral ventricles, polymicrogyria, and abnormal signals in the occipital lobes, suggesting dysmyelination (Fig. 1a–c). Patient 2 is a 2-month-old boy who showed macrocephaly, cutis marmorata of the distal extremities, and hyperextensibility

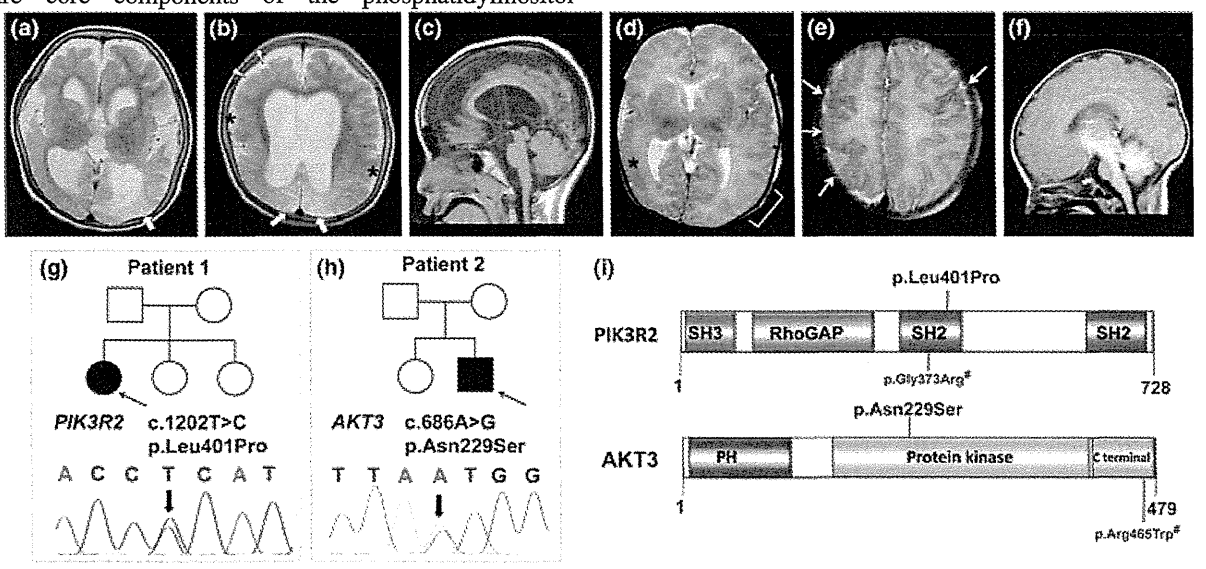

Fig. 1. Magnetic resonance imaging of patient 1 at 6 years of age (**a–c**). (**a, b**) Axial T2-weighted imaging showing enlarged lateral and third ventricles, enlarged extra-axial space, and decreased white matter volume with occipital lobe predominance. Irregular small gyri with areas of cortical thickening compatible with polymicrogyria are observed prominently in the bilateral perisylvian regions (asterisks) and the right frontal lobes (white arrowheads). Abnormal high-intensity signals are seen in the bilateral occipital lobes (thick white arrows). (c) Sagittal T1-weighted imaging showing normal brainstem and cerebellum. Magnetic resonance imaging of patient 2 at 7 days of age (**d–f**). (**d**) Axial T2-weighted imaging at the level of the basal ganglia showing enlargement of the left hemisphere. Polymicrogyria is seen in the perisylvian fissures with right-side dominance, which extends to the right temporal lobe (asterisk). The left parietal cortex shows a blurred border between the gray matter and the white matter (bracket), suggesting dysplasia of cortical development. (**e**) Axial T2-weighted imaging showing polymicrogyria in the right parietal lobe adjacent to the central sulcus (white arrows). (**f**) Sagittal T1-weighted imaging showing a relatively small pontine base. Family pedigrees and causative mutations (**g–i**). (**g**) Patient 1 with MPPH showing a *de novo* heterozygous missense mutation in *PIK3R2* (c.1202T>C, p.Leu401Pro). (h) Patient 2 with MCAP showing a *de novo* missense heterozygous mutation in *AKT3* (c.686A>G, p.Asn229Ser). (i) Distribution of mutations in *PIK3R2* and *AKT3*. SH2, Src homology 2 domain; SH3, Src homology 3 domain; RhoGAP, Rho GTPase-activating protein domain; PH, pleckstrin homology domain. #Reported by Riviere et al. (2).

of the skin. Brain MRI at 7 days showed an asymmetric cerebral hemisphere with right-dominant perisylvian polymicrogyria (Fig. 1d–f), and at 2 months showed a thin corpus callosum and progressive hydrocephalus. These findings were compatible with MCAP.

Whole exome sequencing using DNA extracted from blood leukocytes revealed a *de novo* missense mutation in each patient: p.Leu401Pro in *PIK3R2* (patient 1) and p.Asn229Ser in *AKT3* (patient 2) (Fig. 1g–i). Both mutations were absent from the 6500 eomes sequenced by the National Heart, Lung, and Blood Institute exome project and our 144 in-house control exomes. The read count for mutant alleles possessing p.Leu401Pro in *PIK3R2* was 47.7% (84/176 reads), and that for p.Asn229Ser in *AKT3* was 52.2% (128/245 reads). Therefore, these mutations are likely germline rather than mosaic mutations.

The novel *PIK3R2* mutation (p.Leu401Pro) in patient 1 is within the first Src homology 2 (SH2) domain of the PIK3R2 protein; this domain binds to phosphotyrosine-containing motifs and regulates many aspects of cellular communication (5). Eleven MPPH families have been reported to have a recurrent *PIK3R2* mutation (p.Gly373Arg), which is also located in the first SH2 domain (2). The phenotypes of all 13 cases with the p.Gly373Arg mutation were similar to that of patient 1 (Table 1) (1, 2), implying that impaired function of the SH2 domain is important in the pathogenesis of MPPH. The *AKT3* mutation (p.Asn229Ser) detected in patient 2 with MCAP has been reported in a case of MPPH (2). Furthermore, another case with a different *AKT3* mutation (p.Arg465Trp) was diagnosed with overlapping features of MCAP and MPPH (Table 1). These findings support the notion that the two syndromes have a common genetic basis. Interestingly, somatic mosaicism of an *AKT3* mutation causes hemimegalencephaly, which is similar to MPPH or MCAP (6, 7). Mutation screening of *AKT3* should be considered for patients with MPPH or MCAP as well as those with hemimegalencephaly, for whom pathological tissue is available.

MCAP and MPPH are categorized as overgrowth syndromes, as are Cowden disease and Proteus syndrome that are caused by abnormal activation of the PI3K–AKT pathway, which participates in diverse cellular processes (3, 8). The PI3K–AKT pathway is linked to mammalian target of rapamycin (mTOR) (6), which is a specific molecule for targeted therapeutics (sirolimus or everolimus). Further investigation into potential treatments for overgrowth syndromes is essential.

In summary, we have described two patients with either an *AKT3* or a *PIK3R2* mutation. Our data highlight the importance of the SH2 domain of PIK3R2 in MPPH, and support that MPPH and MCAP have the same genetic origin.

Acknowledgements

We would like to thank the patients and their families for their participation in this study. We thank Aya Narita for technical

Table 1. Phenotypes associated with *PIK3R2* and *AKT3* mutations

Patient (diagnosis)	Patient 1 (MPPH)	13 patients[a] (MPPH)	Patient 2 (MCAP)	LR11-354[a] (MPPH)	LR08-018[a] (overlapping MCAP and MPPH)
Mutation	*PIK3R2* (p.Leu401Pro)	*PIK3R2* (p.Gly373Arg)	*AKT3* (p.Asn229Ser)	*AKT3* (p.Asn229Ser)	*AKT3* (p.Arg465Trp)
Features					
HC SD (age)	+2.6 (1 y 9 m)	+2–8 (8 m–13 y)	+3.0 (2 m)	+6.0 (2 y 5 m)	+5.5 (7.5 m)
Overgrowth	–	2/13	–	–	–
Vascular abnormalities	–	0/13	Skin capillary malformation	–	umbilical hemangioma
Connective tissue dysplasia	–	0/13	+	+	+
Syndactyly	–	0/13	–	–	–
Polydactyly	+	2/13	–	–	–
Epileptic seizures	+	6/9	+	ND	+
Visual impairment	+	ND	–	ND	ND
Neuroimaging features					
Polymicrogyria	+	13/13	+	+	+
Hydrocephalus or ventriculomegaly	+	13/13	+	+	+
CBTE	–	8/13	–	–	+

MPPH, megalencephaly-polymicrogyria-polydactyly-hydrocephalus syndrome; MCAP, megalencephaly-capillary malformation syndrome; HC, head circumference; SD, standard deviation; y, years; m, months; ND, no data; CBTE, cerebellar tonsillar ectopia.

[a] Riviere et al. (2) and Mirzaa et al. (1).

assistance. This work was supported by the Ministry of Health, Labour, and Welfare of Japan (24133701,11103577, 11103340 and 10103235); a Grant-in-Aid for Scientific Research (C) from the Japan Society for the Promotion of Science (24591500); a Grant-in-Aid for Young Scientists from the Japan Society for the Promotion of Science (10013428 and 12020465); the Takeda Science Foundation; the Japan Science and Technology Agency; the Strategic Research Program for Brain Sciences (11105137); and a Grant-in-Aid for Scientific Research on Innovative Areas (Transcription Cycle) from the Ministry of Education, Culture, Sports, Science, and Technology of Japan (12024421).

K. Nakamura[a,b]
M. Kato[b]
J. Tohyama[c]
T. Shiohama[d]
K. Hayasaka[b]
K. Nishiyama[a]
H. Kodera[a]
M. Nakashima[a]
Y. Tsurusaki[a]
N. Miyake[a]
N. Matsumoto[a]
H. Saitsu[a]
[a]Department of Human Genetics
Yokohama City University Graduate School of Medicine
Yokohama, Japan
[b]Department of Pediatrics
Yamagata University Faculty of Medicine
Yamagata, Japan
[c]Department of Pediatrics
Epilepsy Center, Nishi-Niigata Chuo National Hospital
Niigata, Japan
[d]Department of Pediatrics
Kimitsu Chuo Hospital
Chiba, Japan

References

1. Mirzaa GM, Conway RL, Gripp KW et al. Megalencephaly-capillary malformation (MCAP) and megalencephaly-polydactyly-poly microgyria-hydrocephalus (MPPH) syndromes: two closely related disorders of brain overgrowth and abnormal brain and body morphogenesis. Am J Med Genet A 2012: 158A: 269–291.
2. Riviere JB, Mirzaa GM, O'Roak BJ et al. De novo germline and postzygotic mutations in *AKT3*, *PIK3R2* and *PIK3CA* cause a spectrum of related megalencephaly syndromes. Nat Genet 2012: 44: 934–940.
3. Franke TF. PI3K/Akt: getting it right matters. Oncogene 2008: 27: 6473–6488.
4. Tohyama J, Akasaka N, Saito N, Yoshimura J, Nishiyama K, Kato M. Megalencephaly and polymicrogyria with polydactyly syndrome. Pediatr Neurol 2007: 37: 148–151.
5. Liu BA, Jablonowski K, Raina M, Arcé M, Pawson T, Nash PD. The human and mouse complement of SH2 domain proteins – establishing the boundaries of phosphotyrosine signaling. Mol Cell 2006: 22: 851–868.
6. Lee JH, Huynh M, Silhavy JL et al. De novo somatic mutations in components of the PI3K-AKT3-mTOR pathway cause hemimegalencephaly. Nat Genet 2012: 44: 941–945.
7. Poduri A, Evrony GD, Cai X et al. Somatic activation of AKT3 causes hemispheric developmental brain malformations. Neuron 2012: 74: 41–48.
8. Lindhurst MJ, Sapp JC, Teer JK et al. A mosaic activating mutation in *AKT1* associated with the Proteus syndrome. N Engl J Med 2011: 365: 611–619.

Correspondence:
Dr Kazuyuki Nakamura, MD
Department of Pediatrics
Yamagata University Faculty of Medicine
2-2-2 Iida-nishi
Yamagata 990-9585
Japan
Tel: +81-23-628-5329
Fax: +81-23-628-5331
e-mail: kazun-yamagata@umin.ac.jp

Neurogenetics (2014) 15:85–92
DOI 10.1007/s10048-013-0384-7

ORIGINAL ARTICLE

PIGN mutations cause congenital anomalies, developmental delay, hypotonia, epilepsy, and progressive cerebellar atrophy

Chihiro Ohba · Nobuhiko Okamoto · Yoshiko Murakami · Yasuhiro Suzuki · Yoshinori Tsurusaki · Mitsuko Nakashima · Noriko Miyake · Fumiaki Tanaka · Taroh Kinoshita · Naomichi Matsumoto · Hirotomo Saitsu

Received: 2 November 2013 / Accepted: 10 November 2013 / Published online: 20 November 2013

Abstract Defects of the human glycosylphosphatidylinositol (GPI) anchor biosynthetic pathway show a broad range of clinical phenotypes. A homozygous mutation in *PIGN*, a member of genes involved in the GPI anchor-synthesis pathway, was previously reported to cause dysmorphic features, multiple congenital anomalies, severe neurological impairment, and seizure in a consanguineous family. Here, we report two affected siblings with compound heterozygous *PIGN* mutations [c.808T >C (p.Ser270Pro) and c.963G >A] showing congenital anomalies, developmental delay, hypotonia, epilepsy, and progressive cerebellar atrophy. The c.808C >T mutation altered an evolutionarily conserved amino acid residue (Ser270), while reverse transcription-PCR and sequencing demonstrated that c.963G >A led to aberrant splicing, in which two mutant transcripts with premature stop codons (p.Ala322Valfs*24 and p.Glu308Glyfs*2) were generated. Expression of GPI-anchored proteins such as CD16 and CD24 on granulocytes from affected siblings was

Chihiro Ohba, Nobuhiko Okamoto, and Yoshiko Murakami contributed equally

Electronic supplementary material The online version of this article (doi:10.1007/s10048-013-0384-7) contains supplementary material, which is available to authorized users.

C. Ohba · Y. Tsurusaki · M. Nakashima · N. Miyake · N. Matsumoto · H. Saitsu (✉)
Department of Human Genetics, Graduate School of Medicine, Yokohama City University, 3-9 Fukuura, Kanazawa-ku, Yokohama 236-0004, Japan
e-mail: hsaitsu@yokohama-cu.ac.jp

C. Ohba
e-mail: t116017g@yokohama-cu.ac.jp

Y. Tsurusaki
e-mail: tsurusak@yokohama-cu.ac.jp

M. Nakashima
e-mail: mnakashi@yokohama-cu.ac.jp

N. Miyake
e-mail: nmiyake@yokohama-cu.ac.jp

N. Matsumoto
e-mail: naomat@yokohama-cu.ac.jp

C. Ohba · F. Tanaka
Department of Clinical Neurology and Stroke Medicine, Yokohama City University, Yokohama 236-0004, Japan

F. Tanaka
e-mail: ftanaka@yokohama-cu.ac.jp

N. Okamoto
Department of Medical Genetics, Osaka Medical Center and Research Institute for Maternal and Child Health, Izumi 594-1101, Japan
e-mail: okamoto@osaka.email.ne.jp

Y. Murakami · T. Kinoshita
Department of Immunoregulation, Research Institute for Microbial Diseases, Osaka University, Osaka 565-0871, Japan

Y. Murakami
e-mail: yoshiko@biken.osaka-u.ac.jp

T. Kinoshita
e-mail: tkinoshi@biken.osaka-u.ac.jp

Y. Murakami · T. Kinoshita
World Premier International Immunology Frontier Research Center, Osaka University, Osaka 565-0871, Japan

Y. Suzuki
Department of Pediatric Neurology, Osaka Medical Center and Research Institute for Maternal and Child Health, Osaka, Japan
e-mail: yasuzuki@mch.pref.osaka.jp

significantly decreased, and expression of the GPI-anchored protein CD59 in *PIGN*-knockout human embryonic kidney 293 cells was partially or hardly restored by transient expression of p.Ser270Pro and p.Glu308Glyfs*2 mutants, respectively, suggesting severe and complete loss of PIGN activity. Our findings confirm that developmental delay, hypotonia, and epilepsy combined with congenital anomalies are common phenotypes of *PIGN* mutations and add progressive cerebellar atrophy to this clinical spectrum.

Keywords Cerebellar atrophy · Compound heterozygous mutation · Glycosylphosphatidylinositol anchor · *PIGN*

Introduction

Defects of the biosynthetic pathway of the glycosylphosphatidylinositol (GPI) anchor cause broad clinical phenotypes [1]. The products of more than 20 genes in the phosphatidylinositol glycan (PIG) family are involved in GPI biosynthesis, whereas post-GPI-attachment to proteins (PGAP) gene products play a role in the structural remodeling of GPI glycan and lipid portions [2]. Mutations in eight genes involved in GPI biosynthesis and remodeling (*PIGA*, *PIGM*, *PIGN*, *PIGV*, *PIGL*, *PIGO*, *PIGT*, and *PGAP2*) have been identified in individuals with neurological abnormalities [1, 3–5], of which *PIGN* controls the addition of phosphoethanolamine to the first mannose in GPI [6]. To date, only one homozygous *PIGN* mutation has been reported to cause dysmorphic features, multiple congenital anomalies, severe neurological impairment, and seizures in a consanguineous family [7]. Here, we report a family with two affected siblings, possessing compound heterozygous *PIGN* mutations. Detailed clinical information and molecular and functional analyses are presented.

Patients and methods

Patients

We analyzed two affected siblings and their parents. Experimental protocols were approved by the Institutional Review Board of Yokohama City University School of Medicine. Clinical information and peripheral blood samples were acquired from the family members after obtaining written informed consent. Patient clinical features are summarized in Table 1. They showed dysmorphic facial features, developmental delay, intellectual disability, hypotonia, vertical nystagmus, and epilepsy.

Patient 1

This 9-year-old girl was born to nonconsanguineous healthy parents as a second child after 39 weeks of gestation (Fig. 1a). Her birth weight was 3,390 g [+1.40 standard deviation (SD)], body length of 49 cm (−0.03 SD), and head circumference of 35 cm (+1.35 SD). At 1 month of age, she showed vertical nystagmus without eye pursuit. She was hypotonic, and severe developmental delay was evident from early infancy. She was unable to control her head or utter words at 9 years of age. Abdominal echogram revealed bilateral vesicoureteral reflux as a cause of repeated urinary tract infections. Complex partial seizures developed at 8 months of age and were controlled by antiepileptic drugs. Tube feeding by gastrostomy was necessary for poor appetite at the age of 2 years.

Several dysmorphic features (prominent occiput, bitemporal narrowing, epicanthal folds, open mouth, tented upper lip, high arched palate, micrognathia, and deep plantar groove) were noted (Fig. 1b), but hypoplasia was absent from fingers and fingernails. Initial brain magnetic resonance imaging (MRI) at 6 months of age was normal, but cerebellar atrophy was observed at 2 and 6 years of age (Fig. 1c–f).

At present, her height is 122 cm (+1.1 SD), weight of 18.4 kg (−1.2 SD), and head circumference of 51.4 cm (−0.3 SD). Generalized muscle weakness and nystagmus were neurologically recognized. Laboratory examination showed a normal profile, including blood cell count and blood smear, renal and liver function, total bilirubin, uric acid, albumin, serum electrolytes, lactate, pyruvate, ammonia, amino acids, blood gasses, thyroid function, and cerebrospinal fluid study. Her serum alkaline phosphatase (ALP) activity has been normal for her age since infancy. Metabolic disorder screening including organic acid analysis, lysosomal enzymes, and mass spectrometry of transferrin was normal. G-banded analysis showed a normal karyotype (46, XX).

Patient 2

This 2-year-old boy was born after 37 weeks of gestation as a younger brother to patient 1 (Fig. 1a). His birth weight was 3,252 g (+1.3 SD), body length of 50 cm (+1.2 SD), and head circumference of 35 cm (+1.6 SD). He also showed vertical nystagmus at 1 month of age. Complex partial seizures developed at 5 months of age. He was hypotonic, and his developmental milestones were severely delayed with no head control at 1 year and 10 months of age. At present, his height is 92.3 cm (+2.5 SD), weight of 10.9 kg (−0.6 SD), and head circumference of 48.8 cm (+0.4 SD). He showed similar dysmorphic features to patient 1. Brain MRI at 2 months of age revealed no significant abnormalities.

Table 1 Clinical features of patients with *PIGN* mutations

Patient	1	2	Reported by Maydan et al. [7]							
			V-1	V-2	V-4	V-5	V-8	V-9	V-10	Total
Age (years)	9	2	N.D.	Diseased at 14	Diseased at 1	Diseased at 5	Diseased at 3	Diseased at 17	Diseased at 39	
Sex	Female	Male	Male	Male	Male	Female	Female	Female	Male	
Size at birth (percentile)										
Weight (g)	3,390 (90–97)	3,252 (90–97)	3,566 (95)	4,065 (97)	3,850 (95)	3,410 (40)	4,250 (99)	4,300 (98)	4,800 (>99)	
Head circumference (cm)	35 (90)	35 (90–97)	37 (>97)	37 (97)	35.5 (75)	34.5 (10)	N.D.	N.D.	N.D.	
Abnormalities										
Facial features	+	+	+	+	+	+	+	+	+	9/9
Fingers/foot	+	+	+	+	+	-	–	+	+	6/9
Heart	–	–	+	+	+	+	–	+	–	5/9
Urinary tract	+	–	+	+	+	–	–	–	–	4/9
Gastrointestinal tract	GER	–	GER	GER	Anal stenosis	Imperforate anus, ano-vestibular fistula, GER	–	Feeding and swallowing difficulties	Feeding and swallowing difficulties	7/9
Neurological features										
Developmental delay	+	+	+	+	+	+	+	+	+	9/9
Hypotonia	+	+	+	+	+	+	+	+	+	9/9
Nystagmus	+	+	+	+	–	+	–	+	+	7/9
Tremor	+	+	+	+	+	+	+	–	–	7/9
Seizure	+	+	+	–	+	+	+	+	+	8/9
Brain CT	Normal	Normal	Normal	N.D.	Normal	Multiple small subdural hematomas	N.D.	N.D.	N.D.	1/5
Brain MRI				N.D.	N.D.		N.D.	N.D.	N.D.	
Delayed myelination	+	–	–			+				2/4
Thin corpus callosum	–	–	–			+				1/4
Cerebellar atrophy	+	–	Minimal loss of vermis parenchyma			–				1/4
Enlargement of the ventricle	+	–	–			+ (Mild)				2/4

GER Gastroesophageal reflux, *N.D.* not determined

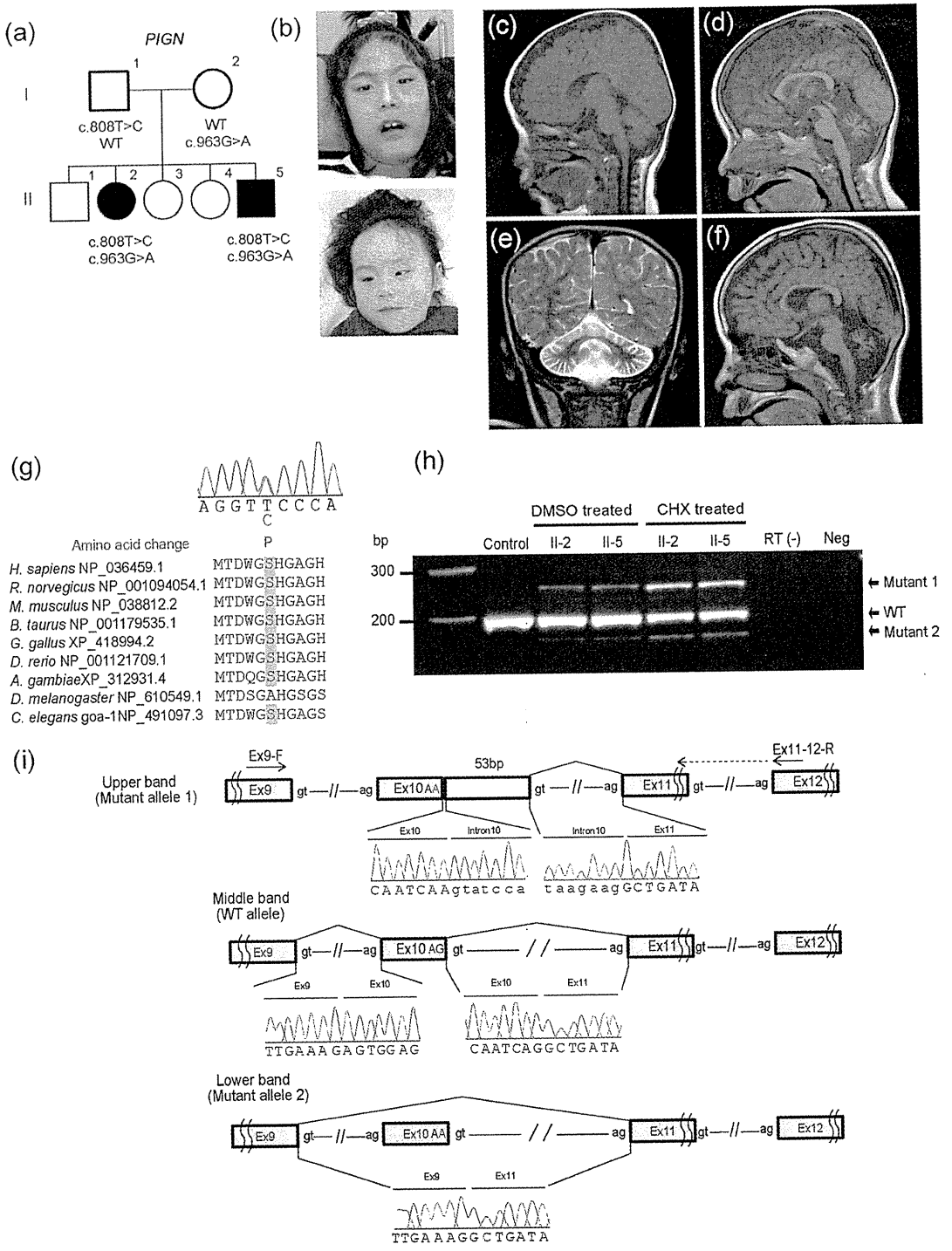

Whole exome sequencing (WES)

Genomic DNA was isolated from peripheral blood leukocytes, captured using the SureSelect Human All Exon v4 Kit (51 Mb; Agilent Technologies, Santa Clara, CA), and sequenced on an Illumina HiSeq2000 (Illumina, San Diego, CA) with 101 bp paired-end reads. Data processing, variant calling, and variant annotation were performed as previously described [8].

◀ **Fig. 1** **a** Familial pedigree and mutations. **b** Photographs of the faces of patient 1 (*upper*) and patient 2 (*lower*). Frontal narrow temporal, frontal bossing, hypertelorism, epicanthal folds, down-slanting palpebral fissures, high nasal bridge, bilateral low set ears, thin philtrum, downturned mouth, and microretrognathia are noted in both patients. **c**, **d**, **f** T1-weighted midline sagittal images and **e** T2-weighted coronal images of patient 1 (**c** at 6 months, **d** and **e** at 2 years, and **i** at 6 years). Progressive vermis atrophy (**c**, **d**, **f**) and hemispheres atrophy (**e**) were observed. **g** Sequence chromatography showing heterozyogous c.808C >T mutation, which alters an evolutionarily conserved amino acid. Homologous sequences were aligned using CLUSTALW. **h** RT-PCR analysis using cDNA of LCLs derived from two patients (II-2 and II-5) and a control. **i** Schematic representation of wild-type (WT) and mutant transcripts and primers used for the analysis. Primer of ex11-12-R spans exons 11 and 12. A single band (200 bp), corresponding to the WT allele, was amplified using control cDNA. Upper and lower bands were detected from patient cDNA. The upper band (253 bp) has a 53-bp insertion of intron 10 sequences, leading to a frameshift mutation. The lower band has a 41-bp deletion of the entire exon 10, also leading to a frameshift mutation

Reverse transcriptase-PCR

Lymphoblastoid cell lines (LCLs) were established from the two patients. RT-PCR using total RNA extracted from LCLs was performed as previously described [9].

Briefly, total RNA was extracted using the RNeasy Plus Mini kit (Qiagen, Tokyo, Japan) from LCLs with or without incubation in 30 μM cycloheximide (CHX; Sigma, Tokyo, Japan) for 4 h. Four micrograms of total RNA was subjected to reverse transcription, and 2 μl cDNA was used for PCR. Primer sequences were ex9-F (5′-TCCTTTAGTCACTTGG GGAGCTGGA-3′) and ex11-12-R (5′-AATCCACAGGAA GGATTCCCACTGA-3′) (Supplementary Table 1). PCR products were electrophoresed on a 10 % polyacrylamide gel and sequenced. PCR bands were purified by the E.Z.N.A. poly-Gel DNA Extraction kit (Omega Bio-Tek, Norcross, GA).

Fluorescence-activated cell sorting (FACS) analysis

Surface expression of GPI-anchored proteins (GPI-APs) was determined by staining cells with Alexa 488-conjugated inactivated aerolysin [fluorescently-labeled inactive toxin aerolysin (FLAER); Protox Biotech, Victoria, BC, Canada] and appropriate primary antibodies: mouse anti-decay accelerating factor (DAF; IA10), −CD16 (3G8), −CD24 (ML5), −CD59 (5H8), and −CD48 (BJ40) followed by a PE-conjugated anti-mouse IgG antibody (3G8, ML5, BJ40, and secondary antibodies; BD Biosciences, Franklin Lakes, NJ). Cells were analyzed by flow cytometry (Cant II; BD Biosciences) with Flowjo software (v9.5.3, Tommy Digital, Tokyo, Japan).

Functional analysis in HEK293 cells

PIGN-knockout cells were generated from HEK293 cells using the CRISPR/Cas System [10]. We obtained the human codon-optimized *Streptococcus pyogenes* Cas9 and chimeric guide RNA expression plasmid pX330 from Addgene (Cambridge, MA). The seed sequence for the SpCas9 target site in *PIGN* exon 4 (CCA-GGTCATGTAGCTCTGATAGC) was selected and a pair of annealed oligos designed according to this sequence and cloned into the *Bbs* I sites of pX330. HEK293 cells were transfected with pX330 containing the target site using Lipofectamine 2000 (Invitrogen, Carlsbad, CA). Cells were stained with anti-CD59 antibody 14 days after transfection, and *PIGN*-knockout clones were obtained by limiting dilution.

PIGN-knockout HEK293 cells (clone PIGNKO2-12) were transiently transfected with a wild-type or mutant (S290P or exon 10 skipping) *PIGN* cDNA cloned into the SRα promoter-driven expression vector pME HA-PIGN. Restoration of the surface expression of CD59, DAF, and GPI-APs was assessed 2 days later by flow cytometry.

Results

WES detected 288 and 292 rare protein-altering and splice-site variants in patients 1 and 2, respectively. We filtered out common single nucleotide polymorphisms (SNPs) that met the following two criteria: variants showing minor allele frequencies ≥1 % in dbSNP 135 and variants found in more than two of our in-house 406 control exomes (Supplementary Table 2). All genes were surveyed for compound heterozygous or homozygous mutations consistent with an autosomal recessive trait, and only *PIGN* (GenBank accession number NM_176787.4) met this criterion, possessing compound heterozygous mutations in two patients. The missense mutation c.808T >C (p.Ser270Pro) was inherited from the patients' father, while c.963G >A is a synonymous mutation inherited from their mother but located at the last base of exon 10 (Fig. 1i). Neither of the two mutations was present in the 6,500 exomes sequenced by the National Heart, Lung, and Blood Institute exome project. In our 406 in-house control exomes, c.808T >C was absent, but c.963G >A was found in one, as a heterozygous mutation. c.808T >C occurred at evolutionary conserved amino acids (Fig. 1g) and was predicted to be pathogenic using online software (Supplementary Table 3). To examine the actual effects of c.963G >A on splicing, RT-PCR was performed (Fig. 1h, i) and a single band (200 bp) corresponding to the wild-type *PIGN* allele was amplified from control LCL cDNA template (Fig. 1h). By contrast, two aberrant faint bands were detected in addition to a wild-type band from patient cDNA (Fig. 1h). Sequencing of the upper aberrant band indicated a 53-bp insertion of intron 10 sequences that had

used a cryptic splice donor site within intron 10, producing a premature stop codon (p.Ala322Valfs*24). Sequencing of the lower band demonstrated the deletion of exon 10 from wild-type *PIGN* mRNA, also producing a premature stop codon (p.Glu308Glyfs*2). Therefore, these two mutant transcripts are likely to be degraded by nonsense-mediated mRNA decay (NMD). In fact, CHX treatment, which inhibits NMD, increased the intensity of the aberrant bands, suggesting that NMD was indeed involved.

To examine the functional impairment of *PIGN* caused by compound heterozygous mutations, the surface expression of various GPI-APs was analyzed by flow cytometry. CD16 and CD24 expression on blood granulocytes was decreased to 26–54 % of normal levels in both patients (Fig. 2a). No abnormal GPI-APs expression was observed on LCLs from either patient (Supplementary Fig. 1).

Transient expression of p.Ser270Pro and exon 10 skipping (p.Glu308Glyfs*2) mutants in *PIGN*-knockout HEK293 cells, in which expression of GPI-APs CD59 was decreased, was confirmed by immunoblotting. Expression of the exon 10 skipping mutant was decreased compared with that of wild-type and p.Ser270Pro mutant (Supplementary Fig. 2). CD59 expression was only partially or hardly restored by the transient expression of p.Ser270Pro and exon 10 skipping mutants, respectively, suggesting severe or complete loss of PIGN activity (Fig. 2b).

Discussion

Herein, we report a second family with *PIGN* mutations that showed clinical features common to a previous affected family, including congenital anomalies, developmental delay, hypotonia, and epilepsy [7]. In addition, nystagmus was an early symptom of patients in this study and was also observed in five of seven patients previously [7]. Of note, progressive cerebellar atrophy was observed in the current patient 1, and this appears to be a novel phenotype associated with *PIGN*

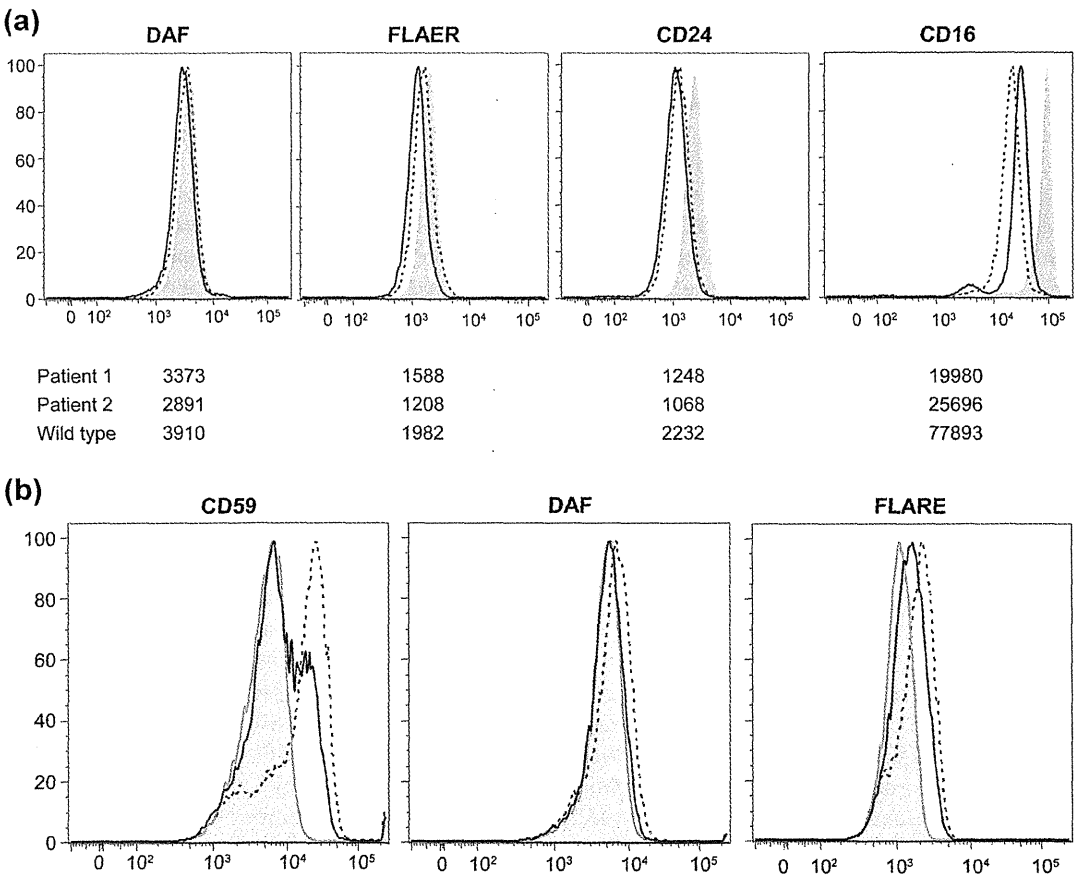

Fig. 2 **a** Surface expression of various GPI-APs on patient granulocytes (patient 1: *dotted lines*, patient 2: *solid lines*), a normal control (*dark shadow*) and an isotype control (*light shadows*). Numbers represent mean fluorescent intensities. Expression of DAF and FLAER in both patients did not significantly change compared with the control. However, CD16 and CD24 expression decreased to 26–54 % of normal levels. **b** *PIGN*-knockout HEK293 cells were transiently transfected with wild type (*dotted lines*) or mutants (exon 10 skipping: *gray line*, p.Ser270Pro: *black line*) of pME HA-PIGN vectors. Empty vector: *dark shadow*, isotype control: *light shadow*. Expression of CD59 was only partially or hardly restored by p.Ser270Pro and exon 10-skipping vectors, respectively

mutations as two patients examined by MRI showed no cerebellar atrophy but only minimal loss of vermis parenchyma in one patient (patient V-1) in the previous report [7].

PIGN is involved in the addition of phosphoethanolamine to the first mannose in GPI [6]. In *Pign*-knockout mouse F9 embryonal carcinoma cells, the first mannose in GPI precursors is not modified by phosphoethanolamine. Nevertheless, further biosynthetic steps continue and the cell surface expression of GPI-anchored proteins is only partially affected [6], suggesting that this modification may not be essential for GPI-anchored protein biosynthesis [6]. By contrast, the *gonzo* mouse line, which harbors the splice donor site mutation in *Pign*, showed abnormal forebrain development resembling holoprosencephaly [11], and patients with *PIGN* mutations show severe phenotypes such as multiple congenital anomalies, neurological impairment, and even lethality [7]; this indicates that particular defects of *PIGN*/*Pign* cause abnormal development both in mice and humans. Although the overall amount of GPI-anchored proteins might not be significantly affected by *PIGN* defects, as revealed by the minimal decrease in DAF and FLAER expression on patient granulocytes in the present study, changes to a subset of GPI-anchored proteins such as CD16 and CD24 can be sufficient to cause severe neurological phenotypes. Additionally or alternatively, GPI-APs expressed on PIGN-defective cells lack the phosphoethanolamine-side branch, and this abnormal structure of the glycan part of the anchor might affect functions of GPI-APs. Functional analysis using neuronal cells may provide novel insights into the pathogenesis of neurological phenotypes caused by *PIGN* mutations.

Seven genes (*PIGA*, *PIGM*, *PIGN*, *PIGV*, *PIGL*, *PIGO*, and *PGAP2*) have been identified as being mutated in patients with neurological abnormalities. Mutations in three of these (*PIGV*, *PIGO*, and *PGAP2*) cause hyperphosphatasia [3, 12–14], suggesting that ALP is a useful marker for suspected GPI anchor-synthesis pathway deficiencies. However, mutations of the other four genes (*PIGA*, *PIGM*, *PIGN*, and *PIGL*) did not cause hyperphosphatasia [7, 14, 15], so clinical diagnosis might be difficult in the absence of specific biomarkers. Even in clinically unsuspected patients, WES may identify mutations in genes involved in the GPI anchor-synthesis pathway. Current advances in next generation sequencing should find more comprehensive answers for unsolved GPI anchor-related diseases.

Acknowledgments We would like to thank patients and their parents for their participation in this study. We also thank Nobuko Watanabe and Kana Miyanagi for technical assistance. This work was supported by the Ministry of Health, Labour, and Welfare of Japan; a Grant-in-Aid for Scientific Research (A), (B), and (C) from the Japan Society for the Promotion of Science (A: 24249019, B: 25293085 25293235, C: 23590363); the Takeda Science Foundation; the Japan Science and Technology Agency; the Strategic Research Program for Brain Sciences (11105137); and a Grant-in-Aid for Scientific Research on Innovative Areas (Transcription Cycle, Exploring molecular basis for brain diseases based on personal genomics) from the Ministry of Education, Culture, Sports, Science, and Technology of Japan (12024421, 25129705).

References

1. Freeze HH, Eklund EA, Ng BG, Patterson MC (2012) Neurology of inherited glycosylation disorders. Lancet Neurol 11(5):453–466. doi:10.1016/s1474-4422(12)70040-6
2. Maeda Y, Kinoshita T (2011) Structural remodeling, trafficking and functions of glycosylphosphatidylinositol-anchored proteins. Prog Lipid Res 50(4):411–424. doi:10.1016/j.plipres.2011.05.002
3. Hansen L, Tawamie H, Murakami Y, Mang Y, ur Rehman S, Buchert R, Schaffer S, Muhammad S, Bak M, Nothen MM, Bennett EP, Maeda Y, Aigner M, Reis A, Kinoshita T, Tommerup N, Baig SM, Abou Jamra R (2013) Hypomorphic mutations in *PGAP2*, encoding a GPI-anchor-remodeling protein, cause autosomal-recessive intellectual disability. Am J Hum Genet 92(4):575–583. doi:10.1016/j.ajhg.2013.03.008
4. Krawitz PM, Murakami Y, Riess A, Hietala M, Kruger U, Zhu N, Kinoshita T, Mundlos S, Hecht J, Robinson PN, Horn D (2013) *PGAP2* mutations, affecting the GPI-anchor-synthesis pathway, cause hyperphosphatasia with mental retardation syndrome. Am J Hum Genet 92(4):584–589. doi:10.1016/j.ajhg.2013.03.011
5. Kvarnung M, Nilsson D, Lindstrand A, Korenke GC, Chiang SC, Blennow E, Bergmann M, Stodberg T, Makitie O, Anderlid BM, Bryceson YT, Nordenskjold M, Nordgren A (2013) A novel intellectual disability syndrome caused by GPI anchor deficiency due to homozygous mutations in *PIGT*. J Med Genet 50(8):521–528. doi:10.1136/jmedgenet-2013-101654
6. Hong Y, Maeda Y, Watanabe R, Ohishi K, Mishkind M, Riezman H, Kinoshita T (1999) Pig-n, a mammalian homologue of yeast Mcd4p, is involved in transferring phosphoethanolamine to the first mannose of the glycosylphosphatidylinositol. J Biol Chem 274(49):35099–35106
7. Maydan G, Noyman I, Har-Zahav A, Neriah ZB, Pasmanik-Chor M, Yeheskel A, Albin-Kaplanski A, Maya I, Magal N, Birk E, Simon AJ, Halevy A, Rechavi G, Shohat M, Straussberg R, Basel-Vanagaite L (2011) Multiple congenital anomalies-hypotonia-seizures syndrome is caused by a mutation in *PIGN*. J Med Genet 48(6):383–389. doi:10.1136/jmg.2010.087114
8. Saitsu H, Nishimura T, Muramatsu K, Kodera H, Kumada S, Sugai K, Kasai-Yoshida E, Sawaura N, Nishida H, Hoshino A, Ryujin F, Yoshioka S, Nishiyama K, Kondo Y, Tsurusaki Y, Nakashima M, Miyake N, Arakawa H, Kato M, Mizushima N, Matsumoto N (2013) *De novo* mutations in the autophagy gene *WDR45* cause static encephalopathy of childhood with neurodegeneration in adulthood. Nat Genet. doi:10.1038/ng.2562
9. Saitsu H, Kato M, Okada I, Orii KE, Higuchi T, Hoshino H, Kubota M, Arai H, Tagawa T, Kimura S, Sudo A, Miyama S, Takami Y, Watanabe T, Nishimura A, Nishiyama K, Miyake N, Wada T, Osaka H, Kondo N, Hayasaka K, Matsumoto N (2010) *STXBP1* mutations in early infantile epileptic encephalopathy with suppression-burst pattern. Epilepsia 51(12):2397–2405. doi:10.1111/j.1528-1167.2010.02728.x
10. Cong L, Ran FA, Cox D, Lin S, Barretto R, Habib N, Hsu PD, Wu X, Jiang W, Marraffini LA, Zhang F (2013) Multiplex genome engineering using CRISPR/Cas systems. Science 339(6121):819–823. doi:10.1126/science.1231143
11. McKean DM, Niswander L (2012) Defects in GPI biosynthesis perturb Cripto signaling during forebrain development in two new mouse models of holoprosencephaly. Biology open 1(9):874–883. doi:10.1242/bio.20121982
12. Freeze HH (2013) Understanding human glycosylation disorders: biochemistry leads the charge. J Biol Chem 288(10):6936–6945. doi:10.1074/jbc.R112.429274

13. Krawitz PM, Murakami Y, Hecht J, Kruger U, Holder SE, Mortier GR, Delle Chiaie B, De Baere E, Thompson MD, Roscioli T, Kielbasa S, Kinoshita T, Mundlos S, Robinson PN, Horn D (2012) Mutations in *PIGO*, a member of the GPI-anchor-synthesis pathway, cause hyperphosphatasia with mental retardation. Am J Hum Genet 91(1):146–151. doi:10.1016/j.ajhg.2012.05.004
14. Almeida AM, Murakami Y, Layton DM, Hillmen P, Sellick GS, Maeda Y, Richards S, Patterson S, Kotsianidis I, Mollica L, Crawford DH, Baker A, Ferguson M, Roberts I, Houlston R, Kinoshita T, Karadimitris A (2006) Hypomorphic promoter mutation in *PIGM* causes inherited glycosylphosphatidylinositol deficiency. Nat Med 12(7):846–851. doi:10.1038/nm1410
15. Johnston JJ, Gropman AL, Sapp JC, Teer JK, Martin JM, Liu CF, Yuan X, Ye Z, Cheng L, Brodsky RA, Biesecker LG (2012) The phenotype of a germline mutation in *PIGA*: the gene somatically mutated in paroxysmal nocturnal hemoglobinuria. Am J Hum Genet 90(2):295–300. doi:10.1016/j.ajhg.2011.11.031

BRIEF COMMUNICATION

Is focal cortical dysplasia sporadic? Family evidence for genetic susceptibility

*†‡[1]Richard J. Leventer, §¶[1]Floor E. Jansen, **††Simone A. Mandelstam, ‡‡Alice Ho, §§Ismail Mohamed, ¶¶Harvey B. Sarnat, ##Mitsuhiro Kato, ***Tatsuya Fukasawa, †††Hirotomo Saitsu, †††Naomichi Matsumoto, ‡‡‡Masayuki Itoh, §§§¶¶¶Renate M. Kalnins, ‡###Chung W. Chow, *†‡A. Simon Harvey, ¶**Graeme D. Jackson, ****Peter B. Crino, ¶Samuel F. Berkovic, and *‡¶**Ingrid E. Scheffer

Epilepsia, 55(3):e22–e26, 2014
doi: 10.1111/epi.12533

Dr Richard Leventer is a consultant pediatric neurologist at the Royal Children's Hospital.

Summary

Focal cortical dysplasia is a common cortical malformation and an important cause of epilepsy. There is evidence for shared molecular mechanisms underlying cortical dysplasia, ganglioglioma, hemimegalencephaly, and dysembryoplastic neuroepithelial tumor. However, there are no familial reports of typical cortical dysplasia or co-occurrence of cortical dysplasia and related lesions within the same pedigree. We report the clinical, imaging, and histologic features of six pedigrees with familial cortical dysplasia and related lesions. Twelve patients from six pedigrees were ascertained from pediatric and adult epilepsy centers, eleven of whom underwent epilepsy surgery. Pedigree data, clinical information, neuroimaging findings, and histopathologic features are presented. The families comprise brothers with focal cortical dysplasia, a male and his sister with focal cortical dysplasia, a female with focal cortical dysplasia and her brother with hemimegalencephaly, a female with focal cortical dysplasia and her female first cousin with ganglioglioma, a female with focal cortical dysplasia and her male cousin with dysembryoplastic neuroepithelial tumor, and a female and her nephew with focal cortical dysplasia. This series shows that focal cortical dysplasia can be familial and provides clinical evidence suggesting that cortical dysplasia, hemimegalencephaly, ganglioglioma, and dysembryoplastic neuroepithelial tumors may share common genetic determinants.

KEY WORDS: Familial, Cortical dysplasia, Ganglioglioma, Hemimegalencephaly, Dysembryoplastic neuroepithelial tumor.

Accepted December 2, 2013; Early View publication Feburary 6, 2014.

*Department of Neurology, Royal Children's Hospital, Melbourne, Victoria, Australia; †Murdoch Childrens Research Institute, Melbourne, Victoria, Australia; ‡Department of Pediatrics, University of Melbourne, Melbourne, Victoria, Australia; §Department of Pediatric Neurology, Rudolf Magnus Institute of Neurosciences, University Medical Center Utrecht, Utrecht, The Netherlands; ¶Epilepsy Research Centre, University of Melbourne, Austin Health, Melbourne, Victoria, Australia; **The Florey Institute of Neuroscience and Mental Health, Melbourne, Victoria, Australia; ††Department of Radiology, University of Melbourne, Melbourne, Victoria, Australia; ‡‡Departments of Pediatrics and Clinical Neurosciences, Alberta Children's Hospital, University of Calgary, Calgary, Alberta, Canada; §§Department of Pediatrics, IWK Health Center, Dalhousie University, Halifax, Nova Scotia, Canada; ¶¶Department of Pediatrics, Pathology, (Neuropathology) and Clinical Neurosciences, University of Calgary Faculty of Medicine, Alberta Children's Hospital, Calgary, Alberta, Canada; ##Department of Pediatrics, Yamagata University Faculty of Medicine, Yamagata, Japan; ***Department of Pediatrics, Anjo Kosei Hospital, Aichi, Japan; †††Department of Human Genetics, Yokohama City University Graduate School of Medicine, Yokohama, Japan; ‡‡‡Department of Mental Retardation and Birth Defect Research, National Institute of Neuroscience, National Center of Neurology and Psychiatry, Tokyo, Japan; §§§Department of Anatomical Pathology, Austin Hospital, Melbourne, Victoria, Australia; ¶¶¶Department of Pathology, University of Melbourne, Melbourne, Victoria, Australia; ###Department of Anatomical Pathology, Royal Children's Hospital, Melbourne, Victoria, Australia; and ****Shriners Hospitals Pediatric Research Center, Temple University, Philadelphia, Pennsylvania, U.S.A.

Address correspondence to Richard J. Leventer, Department of Neurology, Royal Children's Hospital, Flemington Road, Parkville, Vic. 3052, Australia. E-mail: richard.leventer@rch.org.au

[1]These authors contributed equally to this work.

Focal cortical dysplasia (FCD) encompasses a spectrum of cortical abnormalities characterized by dyslamination with or without abnormal cell types. FCDs are among the most common malformations of cortical development (MCDs) and are frequently associated with intractable epilepsy. FCD is often the only congenital abnormality present in the brain or elsewhere, with seizures usually being the sole clinical manifestation. The classification of FCD is based on the presence or absence of features in addition to cortical dyslamination: type I (no abnormal cell types), type II (dysmorphic neurons with or without balloon cells), and type III (type I with another lesion).[1] FCD may accompany hippocampal sclerosis and the "developmental" glioneuronal tumors, ganglioglioma and dysembryoplastic neuroepithelial tumors (DNETs), refining the classification to type IIIa and type IIIb, respectively.[1] A broad developmental classification of MCDs classifies the tubers of tuberous sclerosis complex (TSC), FCD type II, ganglioglioma, hemimegalencephaly, and DNET as all being malformations due to abnormal neuronal and glial proliferation with abnormal cell types.[2]

The etiology of FCD is largely unknown. Although the lesions of FCD (particularly FCD type II) share many imaging and histologic features with cortical tubers of TSC, FCD is usually sporadic, without clinical evidence to support a simple genetic etiology. Mutations in *CNTNAP2* have been reported in children with FCD from Old Order Amish pedigrees.[3] These children differed from most patients with FCD because of mental retardation and macrocephaly, and the imaging findings and histology were not typical of either FCD type I or FCD type II. There have been no other reports of familial FCD. Apart from a single report of a father-son pair with DNET,[4] clinical evidence is lacking to suggest a familial basis for ganglioglioma, DNET, or nonsyndromic hemimegalencephaly, or familial co-occurrence of FCD with hemimegalencephaly, ganglioglioma, or DNET. A role for human papilloma virus (HPV)16 infection in the etiology of FCD type IIb has recently been suggested from studies of resected tissue and a mouse model.[5]

Recent studies of resected tissue from patients with hemimegalencephaly identified de novo somatic mosaic mutations in the genes of the PI3K-AKT3-mTOR (mammalian target of rapamycin) pathway in 9 of 28 patients.[6,7] Evidence from molecular analysis of FCD specimens has led to the hypothesis that these malformations may have a shared pathogenesis, due to abnormalities of mTOR or other cellular pathways that regulate neuronal and glial proliferation.[8] However, until now, there has been no evidence to suggest a link between these disorders from family studies. Here, we report six families, each with two individuals with FCD, ganglioglioma, hemimegalencephaly, or DNET, adding clinical evidence that suggests a shared genetic susceptibility underlying these disorders, and showing for the first time that typical FCD can be familial.

Methods

Families were ascertained by referral to pediatric and adult epilepsy services. Clinical details were obtained from patient interview and medical records. Each institution's human research ethics committee approved the study. Informed consent was obtained from patients or their parents in the case of minors.

Brain magnetic resonance imaging (MRI) was obtained using age-specific epilepsy protocols on 1.5 T or 3 T scanners. Neurologists and neuroradiologists skilled in the detection of MCDs reviewed the MRI scans. Resected tissue was classified by a neuropathologist, according to the proposed system of the International League Against Epilepsy (ILAE) Diagnostic Methods Commission.[1] *TSC1* and *TSC2* mutation screening was performed using DNA extracted from resected brain tissue or whole blood using polymerase chain reaction (PCR) with exon-specific primers for *TSC1* and *TSC2* or by whole exome sequencing techniques.

Results

Six families, each with two affected individuals with seizures and at least one having FCD, were ascertained (pedigrees and selected MRI and neuropathology images: Fig. 1, clinical and imaging details: Table 1, additional MRI and neuropathology images: Fig. S1). All but one patient has undergone epilepsy surgery. None of the patients had clinical features suggestive of TSC, and all patients except family 5 were screened for *TSC1* and *TSC2* mutations. No mutations were identified.

Family 1 comprises brothers with neonatal seizures secondary to right hemisphere FCD type IIa, multifocal in patient 1A and restricted to the right posterior quadrant in patient 1B. The father and paternal uncle of these brothers have each had rare nocturnal seizures without focal features on interictal electroencephalography (EEG). Review of their recent brain MRI studies performed at 3 T revealed no abnormalities. Family 2 includes female 2A with FCD type Ia at the depth of an abnormal branch of the left central sulcus. Her female first cousin 2B had a ganglioglioma in the left superior temporal gyrus. Family 3 includes a female 3A with FCD type IIb in the right anterior temporal pole. Her male cousin 3B had a left middle frontal gyrus DNET. Family 4 includes female 4A with right occipital lobe FCD type IIb. Her nephew 4B had well-controlled focal seizures with a left posterior parietal region lesion on MRI, highly suggestive of FCD that was not removed (see Fig. S1). Family 5 includes a male 5A with an area of FCD type IIb at the depth of an abnormally deep left medial frontal lobe sulcus. His sister 5B had left temporal lobe imaging consistent with both hippocampal sclerosis and FCD in the posteromedial left temporal region, with cortical thickening, blurring of the gray-white

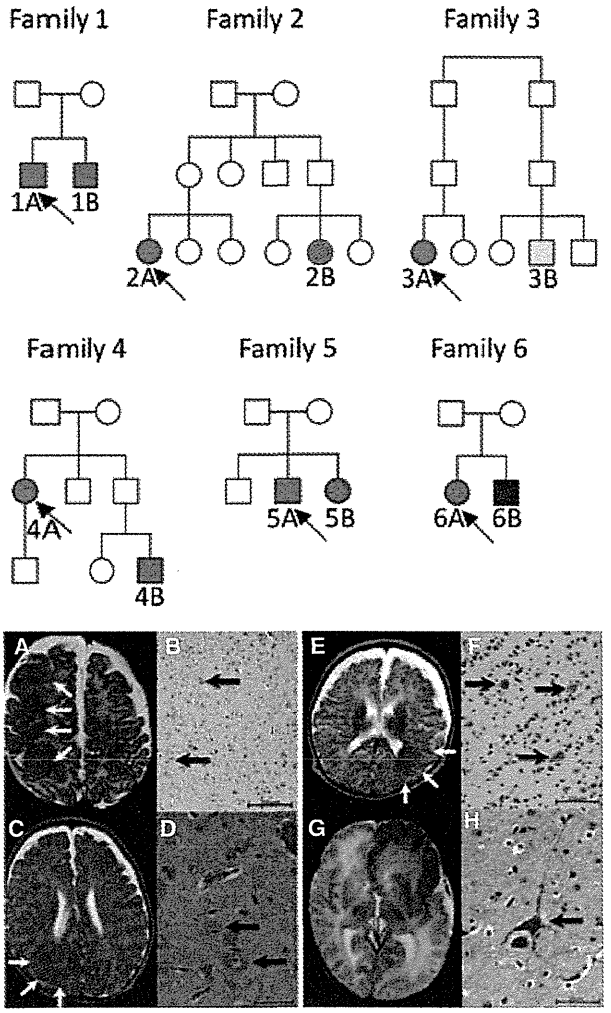

Figure 1.
Pedigrees of the six families and selected brain MRI and neuropathology images of families 1 and 6. **(A)** (top): The proband is marked with an arrow and is assigned "A" and their affected relative is assigned "B." Blue, focal cortical dysplasia; green, ganglioglioma; yellow, DNET; red, hemimegalencephaly. **(B)** (bottom): All MR images are T_2 axial and all pathology images are stained with hematoxylin and eosin (H&E). Family 1 is on the left panel and family 6 is on the right panel. MRI of patient 1A aged 6 weeks (**A**) shows multifocal areas of irregular and thickened cortex, irregular sulcation, and abnormal subcortical signal in the right hemisphere (arrows). MRI of patient 1B aged 14 weeks (**C**) shows an extensive area of irregular and thickened cortex with abnormal signal in the right posterior quadrant (arrows). Histopathology of both patient 1A (**B**) and patient 1B (**D**) showed cortical dyslamination with dense clusters of large dysmorphic neurons (arrows), irregular in orientation, often with prominent Nissl substance and bundles of pinkish fibrillary material in the cytoplasm. Balloon cells were not seen, consistent with FCD type IIa. MRI of patient 6A aged 8 weeks (**E**) shows loss of gray–white matter differentiation, abnormal sulcation, and low signal in the underlying white matter in the posterior left hemisphere (arrows). MRI of patient 6B aged 2 weeks (**G**) shows an enlarged left hemisphere with abnormal sulcation, poor gray–white matter differentiation, and abnormal signal throughout, most prominent in the frontal lobe suggestive of hemimegalencephaly. Histopathology from patient 6A (**F**) showed severe dyslamination and occasional dysmorphic neurons (arrows) consistent with FCD type IIa. Histopathology from patient 6B (**H**) showed abnormal lamination and dysmorphic neurons (arrow) with heterotopic neurons and microcalcification in the white matter. Balloon cells were not seen, consistent with FCD type IIa (within hemimegalencephaly).

matter junction, and high signal on T_2 and fluid-attenuated inversion recovery (FLAIR) images. Histopathology showed hippocampal sclerosis. It was not surprising that no histologic features of FCD were found as there was limited surgical tissue obtained from the abnormal posterior region. Family 6 includes a female 6A with a large area of FCD type IIa in the left posterior quadrant. Her brother 6B had left hemimegalencephaly, containing areas of severe dyslamination and dysmorphic neurons as seen in FCD type IIa.

Discussion

Despite its prevalence, and histopathologic similarity to the tubers in TSC, the molecular causes of FCD remain unknown, and there are no familial cases of typical FCD reported. This suggests that either FCD does not have a genetic basis, or that it does have a genetic basis but occurs sporadically, possibly due to somatic mutations in affected tissue. Evidence to support a relationship between FCD, DNET, hemimegalencephaly, and ganglioglioma has come from a number of sources. First, there are numerous reports of both FCD type I and FCD type II occurring with DNET and ganglioglioma,[9,10] and a report of DNET, ganglioglioma, and FCD coexisting in a "composite lesion" in one patient.[11] Second, an association of FCD, hemimegalencephaly, and ganglioglioma has been suggested from molecular and genetic studies of surgical specimens. These studies show that cytomegaly, seen not only in tubers of TSC but also in hemimegalencephaly, FCD, and ganglioglioma, may reflect aberrant activation of the mTOR and β-catenin signaling cascades, known regulators of cell growth, consequently causing defective control of neuronal and glial proliferation.[12–14] As found in our series, attempts to detect germ line or somatic mutations in *TSC1* and *TSC2* in patients with FCD and related lesions have largely been unsuccessful,[15] suggesting that abnormalities in other genes in the mTOR cascade or related pathways of neuronal proliferation and differentiation may play a role. If we assume that some forms of FCD, DNET, hemimegalencephaly, and ganglioglioma may have a shared etiologic mechanism and timing, then it is reasonable to consider that the occurrence of these lesions in closely related family members may be

Table 1. Clinical data for the six families

Patient	Age	Sz onset	Sz types	Ictal onset	Lesion localization	Age at surgery	Type of surgery	Pathology	Current AEDs	Outcome
1A	16 year	1 d	Tonic, L focal motor	Multifocal R hemisphere	Multifocal R hemisphere	6 m	Hemispherectomy	FCDIIa	NIL	Sz – free
1B	10 y	2 w	L focal motor	R posterior quadrant	R posterior quadrant	10 w and 5 m	Corticectomy + temporo-parietooccipital resection	FCDIIa	NIL	Sz – free
2A	37 y	7 y	R focal motor	L central	L precentral gyrus	27 y	L central corticectomy	FCDIa	LEV	>50% Sz reduction
2B	23 y	8 y	Focal dyscognitive with dysphasia	L temporal	L superior temporal gyrus	14 y	Lesionectomy	GG	NIL	Sz – free
3A	24 y	9 y	Focal dyscognitive with L arm dystonia	R anterior quadrant	R anterior temporal pole	14 y	Lesionectomy	FCDIIb	NIL	Sz – free
3B	28 y	12 y	Aphasia, R facial sensorimotor with generalization	L frontal	L middle frontal gyrus	17 y	Partial lesionectomy	DNET	LEV	>50% Sz reduction
4A	35 y	6 y	Visual aura then L arm dystonia with generalization	R occipital	R occipital	24 y	Lesionectomy	FCDIIb	NIL	Sz – free
4B	12 y	3 y	Focal dyscognitive with vomiting	ND	L posterior parietal	ND	ND	–	VPA	Sz – free
5A	14 y	3 y	Arousal and bipedal hyperkinetic movements	L frontal	L medial superior frontal gyrus	12 y	Lesionectomy	FCDIIb	CBZ, VPA	Sz – free
5B	12 y	4 y	Focal dyscognitive with bilateral hand automatisms +/– generalization	L temporooccipital	L hippocampus and parahippocampal gyrus	5 y	Lesionectomy and anterior temporal lobectomy	HS	CBZ	Sz – free
6A	5 y	1 m	Epileptic spasms and focal motor	L parietal	L posterior quadrant	8 m and 5 y	Focal corticectomy then L posterior quadrantectomy	FCDIIa	LTG, CBZ, PHT	Ongoing Sz
6B	4 m	1 d	Epileptic spasms and multifocal clonic	L frontal	R hemisphere	2 m	Functional hemispherectomy	FCDIIa (HME)	PHT, ZNS	Sz – free

ND, not done; VPA, sodium valproate; LEV, levetiracetam; LTG, lamotrigine; CBZ, carbamazepine; PHT, phenytoin; ZNS, zonisamide; FCD, focal cortical dysplasia; GG, ganglioglioma; DNET, dysembryoplastic neuroepithelial tumor; HME, hemimegalencephaly; HS, hippocampal sclerosis; Sz, seizure; y, year; m, months; L, left; R, right; d, days, w, weeks.

Epilepsia, 55(3):e22–e26, 2014
doi: 10.1111/epi.12533

more than a coincidence and reflective of a shared mechanism and genetic etiology.

If the lesions in our families are caused by genetic mutations giving rise to increased susceptibility, then the question remains as to how different family members may have different lesions, especially in families 2, 3, 4, and 6 in which the proband has FCD but their relative has a developmental tumor or hemimegalencephaly. In TSC, there is significant phenotypic pleiotropy with variation of lesions in family members with the same mutation. More so, within an individual patient with TSC, a mutation can result in both a dysplastic cortical lesion (cortical tubers) and a benign neoplastic lesion (giant cell astrocytoma). Alternatively, lesions in these families could result from "two hits," one causing a nonpathogenic germ line mutation in a cortical development gene carried within the family, and the other causing a somatic mutation of the other allele of that gene within the FCD or other MCD. This hypothesis may explain the sparing of other family members. One may speculate that the nature of the "second hit" may explain the differences in phenotypes within families, with the second mutation either affecting different cellular precursors (i.e., glial vs. neuronal) or affecting precursors at different developmental time points (i.e., early vs. late progenitors).

Identifying the etiology of FCD and related lesions has remained elusive, despite FCD being a relatively common entity. The six families presented herein provide suggestive clinical evidence of a genetic link between FCD, gangliomglioma, hemimegalencephaly, and DNET. It must be acknowledged that FCD and related lesions may occur within the same pedigree as a chance association. Although accurate data on the prevalence of FCD are lacking, we estimate from our own experience that FCD and related lesions are the cause of epilepsy in at most 1 in 100 patients, so the occurrence in multiple families by chance alone would be quite unlikely. Families 1 and 6 in our study, each with siblings with pathologic features of FCD type IIa, are therefore the most convincing pedigrees supporting our hypothesis of a shared genetic susceptibility. Whether this susceptibility extends to other pedigrees that include a family member with FCD and others with MRI-negative epilepsy requires further study, but it is important that in such families the MRI studies of patients with MRI-negative epilepsy be closely scrutinized for subtle lesions. Exploring these relationships further will require molecular exploration of germline mutations in families of interest, in combination with the study of tissue resected at epilepsy surgery for somatic mutations.

Acknowledgments

We would like to thank the patients and their families for participating in this study, Jacinta McMahon for the preparation of pedigree data in Figure 1, and Kate Pope and Rosie Burgess for helping to obtain patient data and DNA samples. This work has been supported by the Victorian Government's Operational Infrastructure Support Program. Funding was provided by the National Health and Medical Research Council of Australia and the Murdoch Childrens Research Institute.

Disclosures or Conflicts of Interest

None of the authors have any conflicts of interest to disclose. We confirm that we have read the Journal's position in issues involved in ethical publication and affirm that this report is consistent with those guidelines.

References

1. Blümcke I, Thom M, Aronica E, et al. The clinicopathologic spectrum of focal cortical dysplasias: a consensus classification proposed by an ad hoc Task Force of the ILAE Diagnostic Methods Commission. *Epilepsia* 2011;52:158–174.
2. Barkovich AJ, Guerrini R, Kuzniecky RI, et al. A developmental and genetic classification for malformations of cortical development: update 2012. *Brain* 2012;135:1348–1369.
3. Strauss KA, Puffenberger EG, Huentelman MJ, et al. Recessive symptomatic focal epilepsy and mutant contactin-associated protein-like 2. *N Engl J Med* 2006;354:1370–1377.
4. Hasselblatt M, Kurlemann G, Rickert CH, et al. Familial occurrence of dysembryoplastic neuroepithelial tumor. *Neurology* 2004;62:1020–1021.
5. Chen J, Tsai V, Parker WE, et al. Detection of human papillomavirus in human focal cortical dysplasia type IIB. *Ann Neurol* 2012;72:881–892.
6. Poduri A, Evrony GD, Cai X, et al. Somatic activation of AKT3 causes hemispheric developmental brain malformations. *Neuron* 2012;74:41–48.
7. Lee JH, Huynh M, Silhavy JL, et al. De novo somatic mutations in components of the PI3K-AKT3-mTOR pathway cause hemimegalencephaly. *Nat Genet* 2012;44:941–945.
8. Crino PB. Focal brain malformations: seizures, signaling, sequencing. *Epilepsia* 2009;50(Suppl. 9):3–8.
9. Saad AG, Jayarao M, Chin LS, et al. Ganglioglioma associated with cerebral cortical dysplasia: an unusual case with extensive leptomeningeal involvement. *Pediatr Dev Pathol* 2008;11:474–478.
10. Takahashi A, Hong SC, Seo DW, et al. Frequent association of cortical dysplasia in dysembryoplastic neuroepithelial tumor treated by epilepsy surgery. *Surg Neurol* 2005;64:419–427.
11. Prayson RA. Composite ganglioglioma and dysembryoplastic neuroepithelial tumor. *Arch Pathol Lab Med* 1999;123:247–250.
12. Ljungberg MC, Bhattacharjee MB, Lu Y, et al. Activation of mammalian target of rapamycin in cytomegalic neurons of human cortical dysplasia. *Ann Neurol* 2006;60:420–429.
13. Samadani U, Judkins AR, Akpalu A, et al. Differential cellular gene expression in ganglioglioma. *Epilepsia* 2007;48:646–653.
14. Aronica E, Boer K, Baybis M, et al. Co-expression of cyclin D1 and phosphorylated ribosomal S6 proteins in hemimegalencephaly. *Acta Neuropathol* 2007;114:287–293.
15. Gumbinger C, Rohsbach CB, Schulze-Bonhage A, et al. Focal cortical dysplasia: a genotype–phenotype analysis of polymorphisms and mutations in the TSC genes. *Epilepsia* 2009;50:1396–1408.

Supporting Information

Additional Supporting Information may be found in the online version of this article:

Figure S1. Selected brain MRI and neuropathology images of families 2, 3, 4, and 5.

FULL-LENGTH ORIGINAL RESEARCH

Early onset epileptic encephalopathy caused by de novo *SCN8A* mutations

*†Chihiro Ohba, ‡Mitsuhiro Kato, §Satoru Takahashi, ¶Tally Lerman-Sagie, #Dorit Lev, **Hiroshi Terashima, **Masaya Kubota, ††Hisashi Kawawaki, ‡‡Mayumi Matsufuji, §§Yasuko Kojima, §§Akihiko Tateno, ##Hadassa Goldberg-Stern, ##Rachel Straussberg, ##Dafna Marom, ***Esther Leshinsky-Silver, *Mitsuko Nakashima, *Kiyomi Nishiyama, *Yoshinori Tsurusaki, *Noriko Miyake, †Fumiaki Tanaka, *Naomichi Matsumoto, and *Hirotomo Saitsu

Epilepsia, 55(7):994–1000, 2014
doi: 10.1111/epi.12668

Chihiro Ohba, a neurologist, is interested in genetic factors causing neuro-developmental disorders.

SUMMARY

Objective: De novo *SCN8A* mutations have been reported in patients with epileptic encephalopathy. Herein we report seven patients with de novo heterozygous *SCN8A* mutations, which were found in our comprehensive genetic analysis (target capture or whole-exome sequencing) for early onset epileptic encephalopathies (EOEEs).

Methods: A total of 163 patients with EOEEs without mutations in known genes, including 6 with malignant migrating partial seizures in infancy (MMPSI), and 60 with unclassified EOEEs, were analyzed by target capture (28 samples) or whole-exome sequencing (135 samples).

Results: We identified de novo *SCN8A* mutations in 7 patients: 6 of 60 unclassified EOEEs (10.0%), and one of 6 MMPSI cases (16.7%). The mutations were scattered through the entire gene: four mutations were located in linker regions, two in the fourth transmembrane segments, and one in the C-terminal domain. The type of the initial seizures was variable including generalized tonic–clonic, atypical absence, partial, apneic attack, febrile convulsion, and loss of tone and consciousness. Onset of seizures was during the neonatal period in two patients, and between 3 and 7 months of age in five patients. Brain magnetic resonance imaging (MRI) showed cerebellar and cerebral atrophy in one and six patients, respectively. All patients with *SCN8A* missense mutations showed initially uncontrollable seizures by any drugs, but eventually one was seizure-free and three were controlled at the last examination. All patients showed developmental delay or regression in infancy, resulting in severe intellectual disability.

Significance: Our data reveal that *SCN8A* mutations can cause variable phenotypes, most of which can be diagnosed as unclassified EOEEs, and rarely as MMPSI. Together with previous reports, our study further indicates that genetic testing of *SCN8A* should be considered in children with unclassified severe epilepsy.

KEY WORDS: *SCN8A*, De novo mutation, Early onset epileptic encephalopathies.

Accepted April 22, 2014; Early View publication June 2, 2014.

*Department of Human Genetics, Graduate School of Medicine, Yokohama City University, Yokohama, Japan; †Department of Clinical Neurology and Stroke Medicine, Yokohama City University, Yokohama, Japan; ‡Department of Pediatrics, Yamagata University Faculty of Medicine, Yamagata, Japan; §Department of Pediatrics, Asahikawa Medical University, Asahikawa, Japan; ¶Pediatric Neurology Unit, Wolfson Medical Center, Holon, Israel; #Metabolic Neurogenetic Clinic, Wolfson Medical Center, Holon, Israel; **Division of Neurology, National Center for Child Health and Development, Tokyo, Japan; ††Department of Pediatric Neurology, Osaka City General Hospital, Osaka, Japan; ‡‡Department of Pediatrics, Japan Community Health Care Organization Kyusyu Hospital, Kitakyushu, Japan; §§Department of Pediatrics, Toho University Sakura Medical Center, Chiba, Japan; ##Department of Neurogenetics, Schneider's Children Medical Center, Petah Tiqwa, Israel; and ***Institute of Medical Genetics, Wolfson Medical Center, Holon, Israel

Address correspondence to Naomichi Matsumoto and Hirotomo Saitsu, Department of Human Genetics, Yokohama City University Graduate School of Medicine, 3-9 Fukuura, Kanazawa-ku, Yokohama 236-0004, Japan. E-mails: naomat@yokohama-cu.ac.jp; hsaitsu@yokohama-cu.ac.jp